Available online at www.sciencedirect.com
ScienceDirect
Radiation Measurements 43 (2008) 580–584
Radiation Measurements
www.elsevier.com/locate/radmeas

Long-term dose measurements applying a human anthropomorphic phantom onboard an aircraft

T. Berger[a,*], M. Meier[a], G. Reitz[a], M. Schridde[b]

[a]DLR—German Aerospace Center, Institute for Aerospace Medicine, Radiation Biology, Linder Hoehe, DE-51147 Cologne, Germany
[b]Lufthansa Cargo AG, DE-65441 Kelsterbach, Germany

Abstract

The exposure of aircrew personnel to cosmic radiation has been considered as occupational exposure in the European Union since the European Council Directive 96/26/EURATOM became effective on 13th May 1996. In Germany the corresponding safety standards for aircrew are regulated by the German Radiation Protection Ordinance, which implemented the European law in 2001. The radiation exposure of the flight crew of the LUFTHANSA group is calculated by the DLR Institute of Aerospace Medicine in Cologne, applying the calculation program EPCARD in the framework of the aircrew dose determination system CALculated and Verified Aviation DOSimetry (CALVADOS). Besides the operational dose calculations, DLR performs measurements at airflight altitudes using active (e.g. TEPC, DOSTEL, etc.) and passive (Thermoluminescence detectors (TLDs), bubble detectors) radiation detectors to verify the calculation codes. Within these activities the project BOdy DOsimetry (BODO) comprised a long-term exposure of a RANDO© anthropomorphic phantom to measure the skin and the depth dose distribution inside a human torso applying TLDs at aviation altitudes for the first time. The torso was flown onboard a LUFTHANSA Cargo aircraft for 3 months from mid of July to mid of October 2004. Over 800 TLDs were positioned for depth dose measurements in the head, the thorax and the abdomen of the torso. In addition dosemeter packages have been distributed on the surface of the torso to measure the skin dose as well as in the transport container and on the flight deck.

Keywords: Aircrew dosimetry; Thermoluminescence detectors; Depth dose distribution; TLD 600; TLD 700

1. Introduction/scope

The atmosphere of our Earth is a massive shield protecting life on Earth from cosmic radiation. At sea level the thickness of the atmosphere is 1033 g/cm^2. At aviation altitudes, ranging from 9 to 12 km, the shielding is reduced to 300–190 g/cm^2, resulting in a higher exposure to cosmic radiation. The radiation field in flight altitudes is composed of the primary radiation components and the secondary products produced by the interaction of the primary particles with the atoms of the atmosphere. The radiation exposure is dependent on the altitude, the latitude—due to the Earth magnetic field—and the solar cycle—due to the variation of the cosmic ray particle flux.

In its Council Directive 96/26/EURATOM (EURATOM, 1996) the European Union declared aircrew members as occupational workers. The European countries have a legal obligation to monitor the radiation exposure of aircrew. Monitoring is mostly achieved by the calculation of route doses applying accredited software. In Germany DLR is calculating the doses for LUFTHANSA in the framework of the CALculated and Verified Aviation Dosimetry (CALVADOS) system (Facius and Meier, 2005). Besides the calculation of route doses, DLR performs regular measurements in flight altitudes with active and passive radiation detector systems. As a part of these measurement campaigns, an anthropomorphic phantom equipped with passive thermoluminescence detectors (TDLs) of the types TLD 600 and TLD 700 was flown onboard a LUFTHANSA Cargo plane to measure the skin and the depth dose distribution for the first time.

* Corresponding author. Tel.: +49 2203 601 31 35; fax: +49 2203 61 970.
E-mail address: thomas.berger@dlr.de (T. Berger).

1350-4487/$ - see front matter © 2007 Elsevier Ltd. All rights reserved.
doi:10.1016/j.radmeas.2007.12.004

2. Materials and methods

2.1. The BODO experiment

From mid-July to mid-October 2004 an anthropomorphic upper torso was flown onboard a LUFTHANSA Cargo plane (see Fig. 1). The torso made of human bones embedded in polyurethane takes into account the different density of the lungs and consists of 28 slices—each 25 mm in height. Three of the slices (#4—head, #16—shoulder, #24—lower torso) were equipped with TLDs ($3.4 \times 3.4 \times 0.9$ mm) of the types TLD 600 (^{6}LiF : Mg, Ti) and TLD 700 (^{7}LiF : Mg, Ti). The TLDs were put into polyethylene tubes. Spacers of polyethylene are used inside the tubes, to enable measurement positions every 25 mm. Fig. 2 shows the flight configuration of the Slice #4. Each measurement point consists of $4 \times$ TLD 700 and $4 \times$ TLD 600 detectors.

Fig. 1. BODO inside the aluminum transport container.

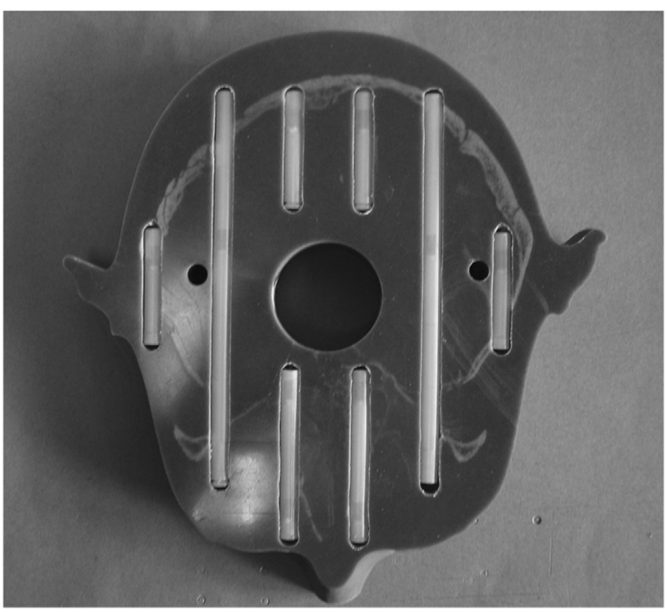

Fig. 2. Slice #4 equipped with TLD tubes for the depth dose measurement into the phantom head.

Besides the TLDs in the phantom, TLDs were distributed in polyethylene holders (seven packages) to measure the skin dose as well as the dose on the aluminum container and in the flight deck (see Table 1 for the location of the packages). Each package contained 8×TLD 600 and 8×TLD 700. Due to storage reasons the phantom was positioned lying on its back for the whole exposure period, which summed up to 900 flight hours during the 3 months.

2.2. Dosemeter readout, calibration and analysis

TLD 600 and TLD 700 produced by Thermo Fisher Scientific Inc.—formerly Harshaw—in the dimensions of $3.4 \times 3.4 \times 0.9$ mm were selected for the project. The TLDs were individually calibrated at the "Material Testing Institute MPA—NRW" with a secondary standard ^{137}Cs-calibration source approved by the National Metrology Institute, PTB, Germany. All readouts were performed with a Harshaw 5500 reader, using flow of pure nitrogen (purity 5.0) with a heating rate $\beta = 5\,°\text{C/s}$ from 100 to 400 °C. For the subtraction of the background signal, each TLD was heated a second time. Data evaluation was performed by using the peak 5 heights of the glowcurves. Annealing was performed for 1 h at 400 °C, following 2 h at 100 °C and slow cool down to room temperature. The total duration of the Body Dosimetry (BODO) experiment was 2160 h, whereas the total duration of the BODO experiment onboard the aircraft was only 900 h. Since the average background dose measured at the laboratory at DLR accounts to 80 nGy/h, the background dose which needs to be subtracted from the flight measurements has been calculated to be 101 μG. All dose values shown are averaged data over four to eight TLD measurements.

Table 1
Absorbed dose values for TLD 600 and TLD 700 for the seven "skin" dose packages. Also given is the γ-equivalent neutron dose derived by subtraction of the TLD 700 from the TLD 600 dose value

Position #	Dose (mGy) TLD 600	Dose (mGy) TLD 700	γ-Equivalent neutron dose (mGy)
#1 Upper torso front	2.39 ± 0.12	1.38 ± 0.02	1.01 ± 0.12
#2 Lower torso front	2.26 ± 0.03	1.40 ± 0.04	0.86 ± 0.05
#3 Lower torso right side	2.35 ± 0.02	1.32 ± 0.05	1.03 ± 0.06
#4 Lower torso left side	2.26 ± 0.08	1.37 ± 0.02	0.89 ± 0.08
#5 Aluminum box lower torso	2.10 ± 0.08	1.43 ± 0.04	0.67 ± 0.09
#6 Aluminum box torso head	2.18 ± 0.03	1.45 ± 0.03	0.73 ± 0.04
#7 Flight deck	2.54 ± 0.08	1.48 ± 0.03	1.07 ± 0.09

3. Results and discussion

3.1. Skin dose packages

Fig. 3 shows the glowcurves of TLD 600 and TLD 700 dosemeters for the package #7 (flight deck). The glowcurves are already normalized to the same γ-calibration factor. The difference in the glowcurve structure—peak 5 and the high-temperature peaks in TLD 600—is due to the contribution of thermal, via the $^{6}Li(n,\alpha)^{3}H$ reaction, and epithermal neutrons, which deposited their dose in the material.

The subtraction of the TLD 700 from the TLD 600 signal therefore gives a "net glowcurve" only based on the contribution from neutrons. This "net glowcure" resulting in a γ-equivalent neutron dose is also shown in Fig. 3.

Table 1 gives the absorbed dose values for the seven "skin" dose packages for TLD 600 and TLD 700 detectors as well as the derived γ-equivalent neutron dose. In comparison to the two packages mounted directly on the aluminium container, the four packages mounted as "skin" dose detectors on the phantom showed a higher contribution of the neutron dose—due to albedo neutrons from the phantom.

To gain more information about the "neutron dose", the TLD 600 and TLD 700 detectors were calibrated at the CERF—High Energy Reference Field at CERN in October 2006. This field resembles the neutron spectra at aviation altitudes (Mitaroff and Silari, 2002). By calibration of TLD 600 and TLD 700 detectors in the field, an average calibration factor of $3.8 \pm 0.32\,\mathrm{Sv/Gy}$ was calculated. Using this calibration factor the neutron dose equivalent, based on the γ-equivalent neutron dose, for package #7 was derived with $4.07 \pm 0.70\,\mathrm{mSv}$. Adding the low-LET component from the TLD 700 reading the total dose equivalent accounts to 5.4 mSv. Calculations with EPCARD (Mares and Schraube, 2002) for the flight routes revealed an effective dose of 4.2 mSv. The use of very small radiation detectors overestimates the dose but gives a good first dose assessment applying these detector systems.

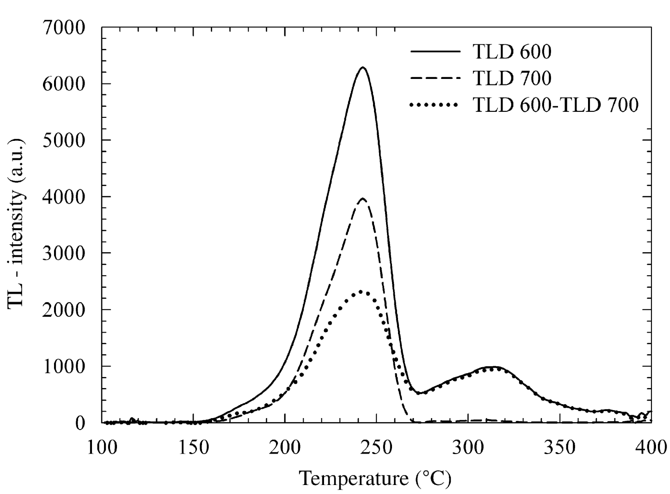

Fig. 3. TLD 600 (solid line) and TLD 700 (long dashed line) glowcurves (normalized on the same gamma calibration factor) as well as NET neutron glowcurve (TLD 600—TLD 700) (dotted line) of the skin dose packages.

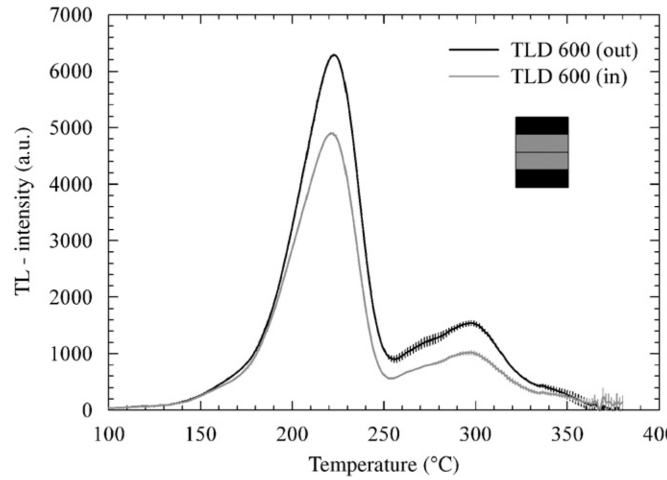

Fig. 4. Glowcurves for TLD 600 inside the phantom (TLD 600 (out) in black and TLD 600 (in) in gray).

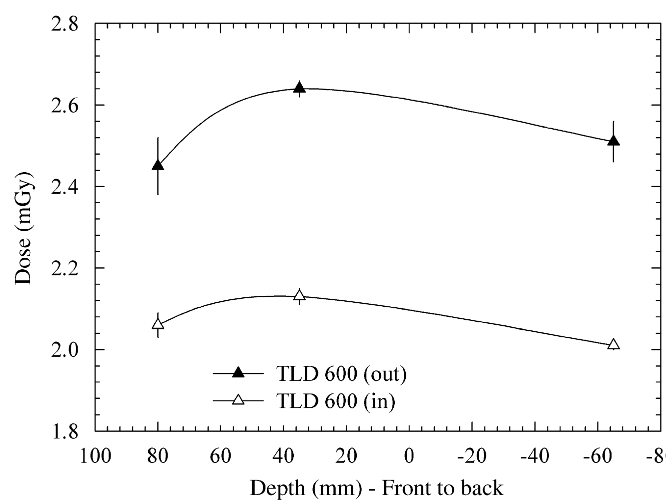

Fig. 5. Depth dose distribution for TLD 600 (out) and TLD 600 (in) for Slice #4 (front to back).

3.2. Phantom depth dose

The TLDs for the measurement of the depth dose distribution are arranged in stacks of 4×TLD 600 followed by 4×TLD 700 detectors inside the tubes. This arrangement and the glowcurves of the TLD 600 detectors are shown in Fig. 4. The two TLD 600 detectors in the middle of the stack (TLD 600 (in)) show a lower signal than the two detectors at the outside of the stack (TLD 600 (out)). This is explained by the high interaction cross-section of TLD 600 detectors and the high absorption probability of these detector material to thermal neutrons, respectively (Horowitz et al., 1976). Therefore, a big part of the thermal neutron contribution will already be absorbed in the outer TLDs, though there can still be a small contribution from thermal neutrons coming from the side for the inner TLDs. To highlight this feature the depth dose distribution for TLD 600 detectors for Slice #4 is shown in Fig. 5 for both the outside

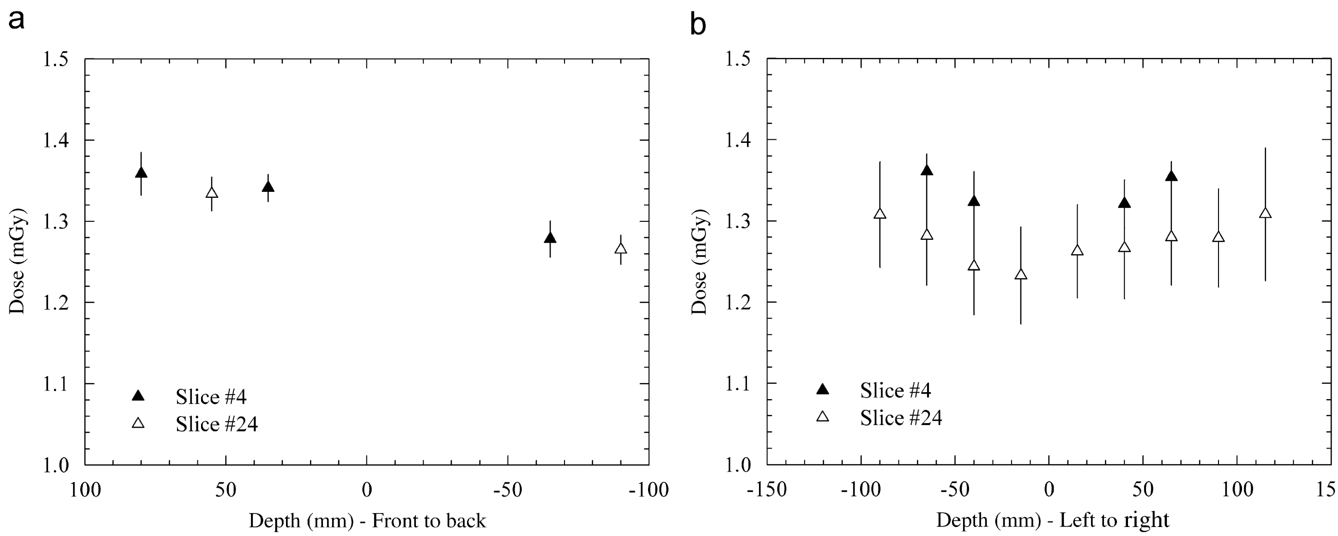

Fig. 6. (a) Depth dose distribution for TLD 700 for Slices #4 and #24 (front to back) and (b) depth dose distribution for TLD 700 for Slices #4 and #24 (left to right).

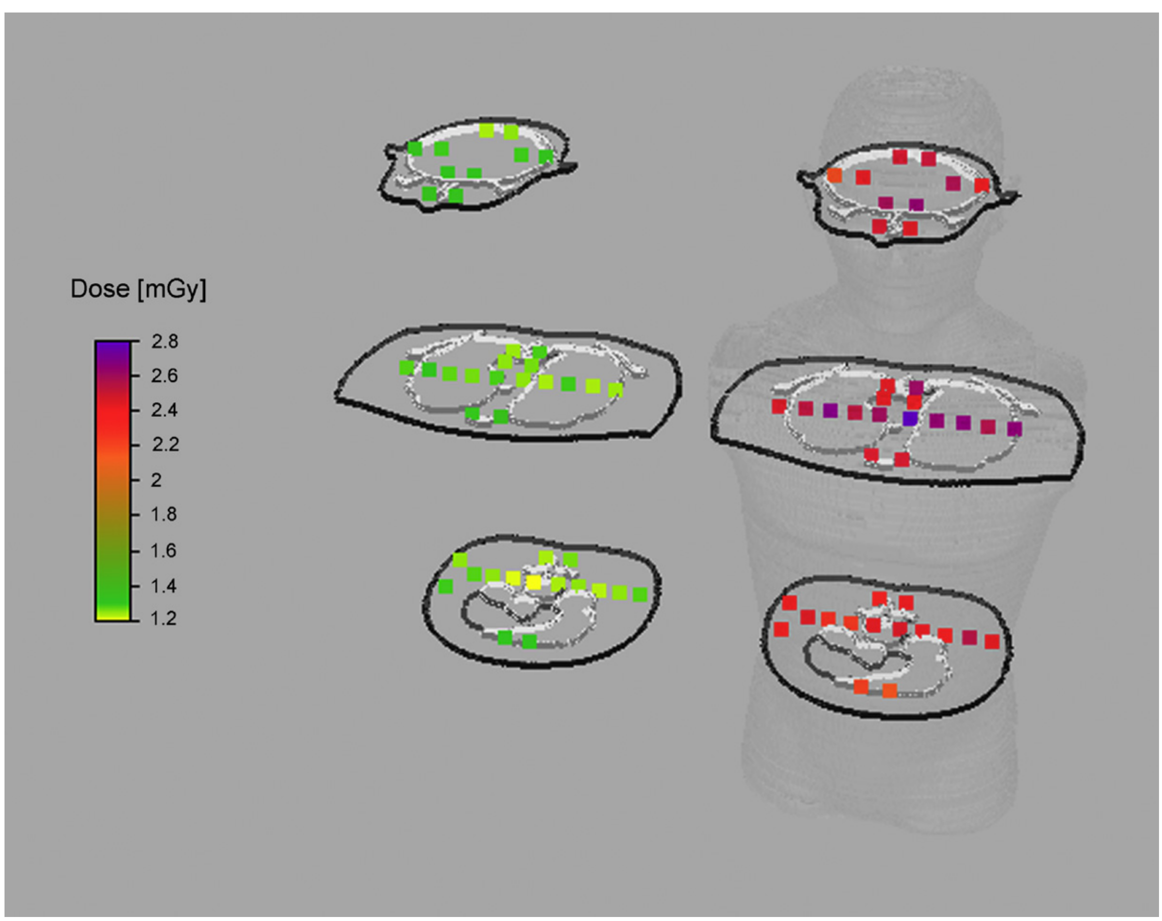

Fig. 7. The three-dimensional dose distribution TLD 700 (left) and TLD 600 (right).

and the inside TLD 600 detectors. A difference in dose up to ∼ 25% was observed. For the investigations of the depth dose measurement, only the dose values for the TLD 600 (out) were taken into account.

The depth dose distributions for the TLD 700 detectors for the Slices #4 (head) and #24 (lower torso) are shown in Figs. 6a and b. Fig. 6a shows the depth dose distribution from the front to the back of the phantom. Due to storage reasons the phantom was lying on its back for the whole exposure period. This is reflected in Fig. 6a, where the dose decreases with depth—from the front side to the back side. For the dose distribution from the left to the right side (Fig. 6b), a decrease into depth is observed for both Slices #4 and #24.

Fig. 7 shows the depth dose distribution for the three slices equipped with TLDs—a total number of 62 measurement positions for TLD 700 (left side) and TLD 600 (right side) in a three-dimensional way. In addition, the outline of the phantom is shown.

While the dose for the TLD 700 detectors lies around 1.2–1.4 mGy, the dose from the TLD 600 detectors increases with depth due to a thermalization of the neutron field inside the body up to 2.8 mGy in Slice #16. For TLD 700 readings, the skin dose values still act as "conservative" estimation of dose—considering TLD 700 as "low-LET" detector. The increase of the TLD 600 data with depth gives information about the thermal and epithermal neutron components but cannot imply any change in the high-energetic part of the neutron spectra.

4. Conclusion

For the first time an anthropomorphic phantom was flown for long time radiation exposure in a LUFTHANSA Cargo plane. Depth dose distribution as well as skin dose were measured with a combination of TLD 600 and TLD 700 detectors. While the TLD 700 dose readings decrease into the depth of the phantom, an increase in the TLD 600 readings due to an increased contribution of thermalized neutrons was observed. For a better understanding—especially of the neutron component as well as a possible change in neutron spectra inside the body—further investigations will include a combination of active and passive radiation detectors in and outside the phantom.

Acknowledgments

The authors want to thank the colleagues from LUFTHANSA Cargo for their help and support during the experiment.

References

EURATOM, 1996. Council Directive 96/26/EURATOM of 13 May 1996 laying down basic safety standards for the protection of the health of workers and the general public against the dangers arising from ionising radiation. Off. J. Eur. Communities L 159.

Facius, R., Meier, M., 2005. Radiation Protection for Flight Crew—Personnel Guidelines for the Instruction of Flight Crew in Accordance with the German Radiation Protection Ordinance. Deutsche Lufthansa AG,

Horowitz, Y.S., Dubi, A., Ben Shahar, B., 1976. Self-shielding factors for TLD-600 and TLD-100 in an isotropic flux of thermal neutrons. Phys. Med. Biol. 21, 976–979.

Mares, V., Schraube, G., 2002. EPCARD—European program package for the calculation of aviation route doses. GSF-Report 08/02, Neuherberg.

Mitaroff, A., Silari, M., 2002. The Cern–EU high energy reference field (CERF) facility for dosimetry at commercial flight altitudes and in space. Radiat. Prot. Dosim. 102, 7–22.